

Small-Angle Neutron Scattering from Labeled Single-Wall Carbon Nanotubes

Barry J. Bauer,* Erik K. Hobbie, and Matthew L. Becker

Polymers Division, National Institute of Standards and Technology, Gaithersburg, Maryland 20899

Received December 21, 2005; Revised Manuscript Received February 1, 2006

ABSTRACT: Small-angle neutron scattering (SANS) is used with the “high-concentration” method to extract single-particle scattering from single-wall carbon nanotubes (SWNTs). The SWNT material was labeled by covalently attaching $-C_4H_9$ or $-C_4D_9$ groups by use of free radical chemistry. Mixtures of SWNT- C_4H_9 and SWNT- C_4D_9 were dispersed in D_2O containing 1% sodium lauryl sulfate- d_{23} (SLS) by use of sonication. SLS matches the neutron contrast of D_2O so that all of the SANS is due to the labeled SWNT. Thermogravimetric analysis shows that mass fractions of butyl groups attached to the SWNT- C_4H_9 and the SWNT- C_4D_9 were well matched. The scattering had a power law of -2.5 , which is characteristic of a “particle” made of clustered SWNTs. The clustering seen in SWNT scattering is due to collections of SWNTs that do not exchange in a dynamic equilibrium with other nanotubes.

Introduction

Single-wall carbon nanotubes (SWNTs) have a variety of potential applications in materials due to their outstanding mechanical, electrical, optical, and thermal properties.¹ However, current SWNT synthetic methods produce masses of nanotubes that need to be separated from each other to produce individual nanotubes that can be sorted and manipulated.

Many of the potential applications of SWNTs involve their dispersion in liquid or solid matrices.² Several schemes have been developed to promote SWNT dispersion which have demonstrated the ability to form stable suspensions that do not settle out over long time periods. The nature of the dispersion on a size scale comparable to the SWNTs is of great importance to device fabrication, which is the ultimate goal, requires the facile manipulation of individual tubes. While techniques such as microscopy can show the existence of individual tubes, small-angle scattering is capable of determining the average dispersion of large collections of SWNTs.

Small-angle scattering can be used to measure the structure of complex objects on several length scales.³ Fractal objects contain a self-similarity over a range of sizes. If the structure is viewed at magnifications that probe different size scales, the structure appears the same. An example is a very long and very thin rod. For a range of sizes between the rod length and rod diameter, the structure appears similar, a straight line of negligible thickness that extends to the limit of viewable distance.

Figure 1 shows a collection of model structures and the resultant small-angle scattering. The log–log plots are of the intensity of scattered radiation at a characteristic scattering vector, $q = 4\pi \sin(\theta/2)/\lambda$, where θ is the angle of the scattered radiation having a wavelength λ . A relative size scale, d , is probed by the q value as $d = 2\pi/q$. The plots are a series of power law regions that vary within the region as $I(q) \propto q^{-\alpha}$, where $I(q)$ is the scattered intensity at q and α is the characteristic power law. They are shown as linear regions on a log–log plot, connected by characteristic lengths. For example, the rod plot transitions from a power law of 0 to -1 at q value related by the radius of gyration, R_g . Other types of structures

have a transition at low q dependent on the R_g of the total structure, but the power law depends on the form of the structure, e.g. a self-avoiding polymer chain has a slope of $-5/3$ and a Gaussian chain -2 . Occasionally, structures have a transition relating to an internal size. For example, if a long rod is broken along its length, forming a series of connected rigid segments, it appears as a rod at lengths below its “persistence length” and as a self-avoiding walk at longer length scales. There is a transition of power law slope from $-5/3$ to -1 at q value dependent on the persistence length. Figure 1 shows idealized structures; for example, a self-avoiding polymer chain can appear as a broken rod at a length scale smaller than the persistence length and as a hard surface at an even smaller length. A typical scattering experiment only covers a limited range of q and hence only measures certain fractal regions.³

Two important structures are shown on the right-hand side of Figure 1. If a number of rods or flexible chains are brought together as an aggregate, a structure is formed that has branching points. The power law associated with such a structure is generally between $(-2$ and $-3)$ depending on the type of joining. At higher q , the internal structure of each chain is seen producing slopes of -1 for rods and $-5/3$ for flexible chains. It is important to note that a slope of between $(-2$ and $-3)$ for a chain molecule such as a polymer or a SWNT strongly suggests aggregation. Power laws between $(-2$ and $-3)$ are possible for certain objects such as a large flat disk or a disk with a convoluted surface, but it is unlikely that SWNTs could form such objects.

Small-angle X-ray scattering (SAXS)^{4,5} and small-angle neutron scattering (SANS)^{6–9} have been used to measure the structure of SWNT dispersions. All of the previous work has found power law scattering in the region $q < 0.01 \text{ \AA}^{-1}$ with $2 < \alpha < 3$. This is characteristic of branched or aggregated rods or chains. Schaefer et al.^{4,5} describe the scattering as “network of tubes”. The reported scattering seems dominated by clusters, even though individual chains may also be present in the mix.

The aggregates could be either remnants from the synthesis that have never become separated by the dispersion process or associations in dynamic equilibrium with individual tubes. SANS has the ability of distinguishing these two cases. Figure 2 is a diagram of two SWNT materials, identical in size, shape,

* Corresponding author: e-mail barry.bauer@nist.gov.

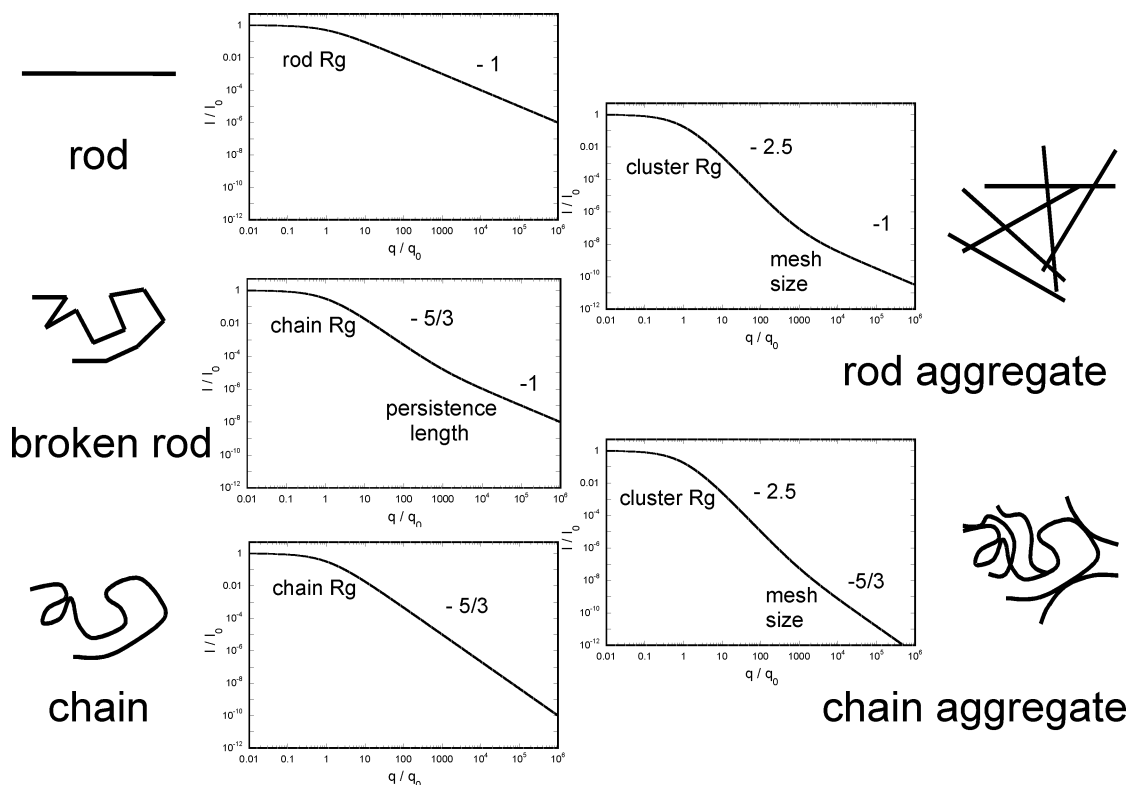


Figure 1. Power law scattering from fractal objects.

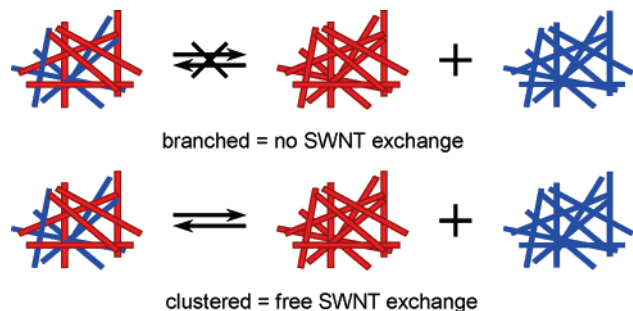


Figure 2. Schematic outlining the possible mechanisms for exchange of SWNT components. Clusters are weak aggregates and can exchange tubes. Branches do not exchange aggregated components, only unattached pieces exchange.

and thermodynamic interactions, but differing in neutron contrast factor. In this schematic, the aggregates are shown as randomly oriented rods. Individual clusters shown by the red or blue diagrams would each produce the scattering that has been reported. If dynamic equilibrium exists, a mixture of the two would mix randomly on the level of individual chains, producing scattering that is distinguished easily from the case in which mixing occurs on the level of permanently branched aggregates. To distinguish these two cases, the term “cluster” will be used to describe weakly associated SWNTs which readily exchange and “branch” will be used for permanently bonded SWNTs that remain physically attached during the duration of the measurement. If ultrasonication mixes the SWNTs on a single-tube level, they would be “clustered”.

SANS can extract single-particle scattering from such mixtures¹⁰ by the use of what is commonly referred to as the “high-concentration” method. Two samples are prepared identical in structure but having different atomic isotopes and therefore different neutron contrast as is represented by scattering cross section. While, in principle, SWNTs could be made of ¹²C and

¹³C, the neutron contrast between these isotopes is quite small compared to the difference between ¹H (hydrogen) and ²H (deuterium). SWNTs themselves contain no hydrogen, so deuterium substitution cannot be used on them alone. However, several methods of covalently attaching hydrocarbons have been reported.¹¹ Billups¹² uses free radical chemistry to attach alkyl groups that supply the required hydrogen for the high-contrast technique. While this could conceivably change the shape and association of the nanotubes, it is the only practical way of labeling the tubes for the high-concentration method. The Billups method¹² was chosen as an example of chemical modification, but many others modification schemes would be appropriate.¹¹

Scattering from concentrated mixtures has contributions from single-particle correlations, $P(q)$, and interparticle correlations, $Q(q)$. $P(q)$ contains information on molecular mass, size, stiffness, branching, etc., and $Q(q)$ contains information on clustering, ordering, etc. Equation 1 defines $P(q)$ and $S(q)$, where \vec{q} is the scattering vector, $(\vec{r}_m - \vec{r}_n)$ is the vector between the position of the m and n units, and Z is the number of units per SWNT. The variables are based on the naming convention by Roe.¹⁰

$$P(q) \text{ or } S(q) = \frac{1}{Z^2} \left\langle \sum_{m=1}^Z \sum_{n=1}^Z \exp[i\vec{q} \cdot (\vec{r}_m - \vec{r}_n)] \right\rangle \quad (1)$$

$P(q)$ and $Q(q)$ differ in that the summed units of the $P(q)$ are all on the same connected structure while $Q(q)$ sums the values from all units on unconnected structures. For a mixture of identical SWNTs, SWNT-h and SWNT-d, with differing contrast factors, σ_H and σ_D , dispersed in a medium with contrast factor σ_S , for a SWNT mixture with a molecular mass of M_W and a mole fraction of ¹H h and ²H d of x_H and x_D and a total volume fraction in the medium, ϕ , K is an instrumental constant that is not calculated since only the relative values of $P(q)$ and

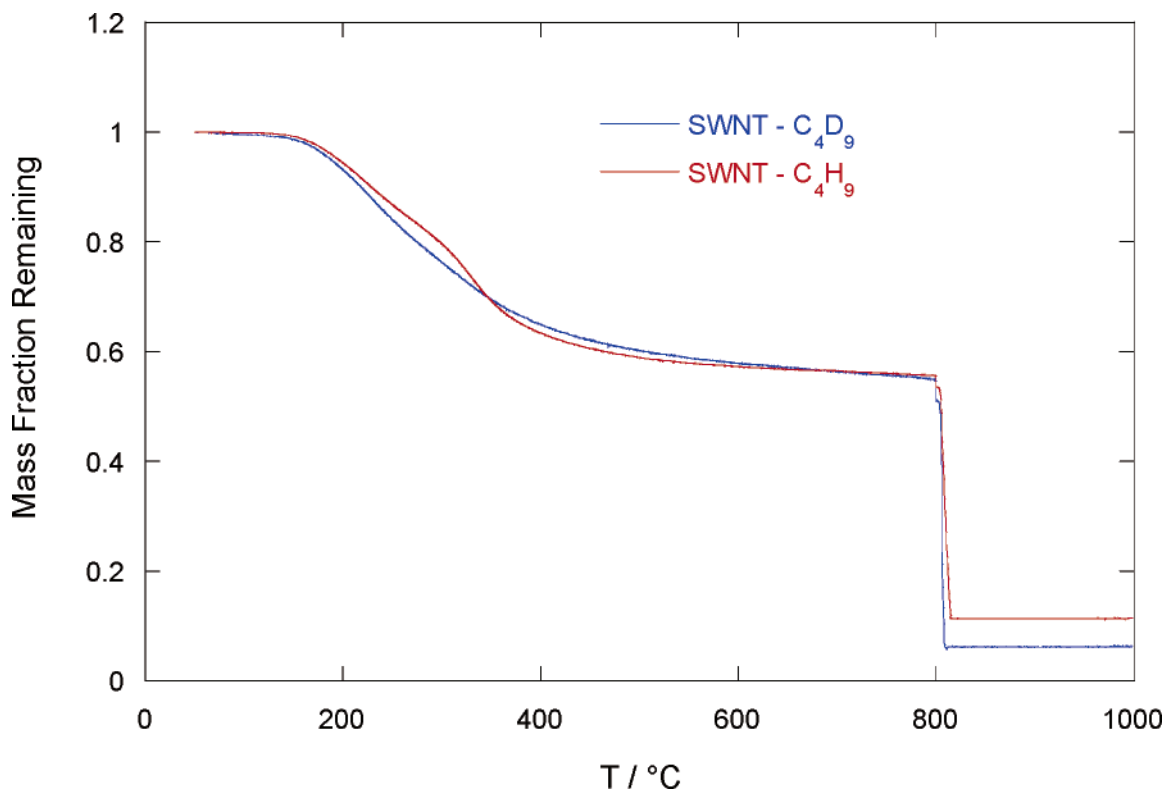


Figure 3. Thermogravimetric analysis of butyl-grafted SWNTs.

$I(q)$ are of interest. The scattered intensity, $I(q)$, is given by

$$I(q) = KM_w[(x_D(\sigma_D - \sigma_S)^2 + x_H(\sigma_H - \sigma_S)^2)P(q) + (x_D\sigma_D + x_H\sigma_H - \sigma_S)^2\phi Q(q)] \quad (2)$$

By varying the relative amounts of the SWNT-d and SWNT-h, the single-particle and interparticle contributions can be calculated independently. A series of scattering experiments are carried out at constant ϕ but varied x to produce a series of equations to fit both $P(q)$ and $Q(q)$.

Experimental Section

SWNTs were obtained from Carbon Nanotechnologies Inc.¹³ The chemical modification reaction was carried out according to the procedure of Billups et al.¹² The nanotubes were sonicated in benzene for 30 min using a bath sonicator. Butyl iodide, C_4H_9I (Aldrich Chemical, 99%), or butyl- d_9 iodide, C_4D_9I (CDN Isotopes, 99.3%), was added along with benzoyl peroxide, and the mixture was refluxed for 24 h. The reaction product was poured into methanol and centrifuged to remove solids. The solids were (dispersed, precipitated, and centrifuged) five times to remove unreacted material and dried in a vacuum.

Dispersions for SANS and ultraviolet–visible–near-infrared (UV–vis–NIR) were made by sonicating the grafted tubes in a 1% by mass fraction solution of sodium lauryl sulfate- d_{23} (SLS) in D_2O at 1 mg/mL SWNT concentration. An ultrasonic processor with a 3 mm tip was used for 2 h at 10 W. The dispersions were centrifuged for 10 min, and the top layer was removed. UV–vis–NIR measurements of the top layer showed that the concentration was lowered to about 0.4 mg/mL.

The thermogravimetric analysis (TGA) was done with a TA Instruments Q500 using a ramp from 50 to 800 °C at 10 °C/min in nitrogen, isothermal at 800 °C for 30 min, and then a final ramp from 800 to 1000 °C at 10 °C/min in air. The ultraviolet, visible, near-infrared spectroscopy (UV–vis–NIR) was done with a Perkin-

Elmer Lambda 9. Small-angle neutron scattering (SANS) was performed on the 30 m NG7 instrument at the National Institute of Standards and Technology (NIST) Center for Neutron Research (NCNR).

The relative uncertainties reported are one standard deviation, based on the goodness of the fit. Total combined uncertainties from all external sources are not reported, as comparisons are made with data obtained under the same conditions. In cases where the limits are smaller than the plotted symbols, the limits are left out for clarity.

Results

TGA of the two SWNT materials is shown in Figure 3. The mass loss in the first stage in nitrogen represents the mass fraction of butyl groups attached to the SWNT and gives $f_H = 0.47$ and $f_D = 0.49$ for the SWNT- C_4H_9 and SWNT- C_4D_9 , respectively. The second stage in air burns off the SWNT, leaving only Fe_2O_3 . The iron catalyst residue accounts for less than 1 atomic % and is negligible in the SANS. While the close similarity of the butyl substitution is desirable, the high-concentration technique could be applied to samples possessing a greater difference, as long as the overall contrast factor is known.

Figure 4 shows the UV–vis–NIR absorption of the dispersions in D_2O with SLS surfactant have lost the transitions due to conversion of sp^2 carbons to sp^3 . These results are consistent with previous findings.¹² Also shown in Figure 4 are spectra of dispersions of unreacted SWNTs, dispersed with surfactant (sodium dodecyl benzenesulfonate),⁹ and wrapping polymer (DNA).^{14,15} The unreacted SWNTs show van Hove transitions typical of SWNTs that have retained the sp^2 structure. Therefore, both TGA and UV–vis–NIR demonstrate that relatively large numbers of butyl groups have been covalently bonded to the SWNTs.

SANS measurements were made on two samples containing 100% SWNT-h and 100% SWNT-d. The SLS- d_{23} has the same

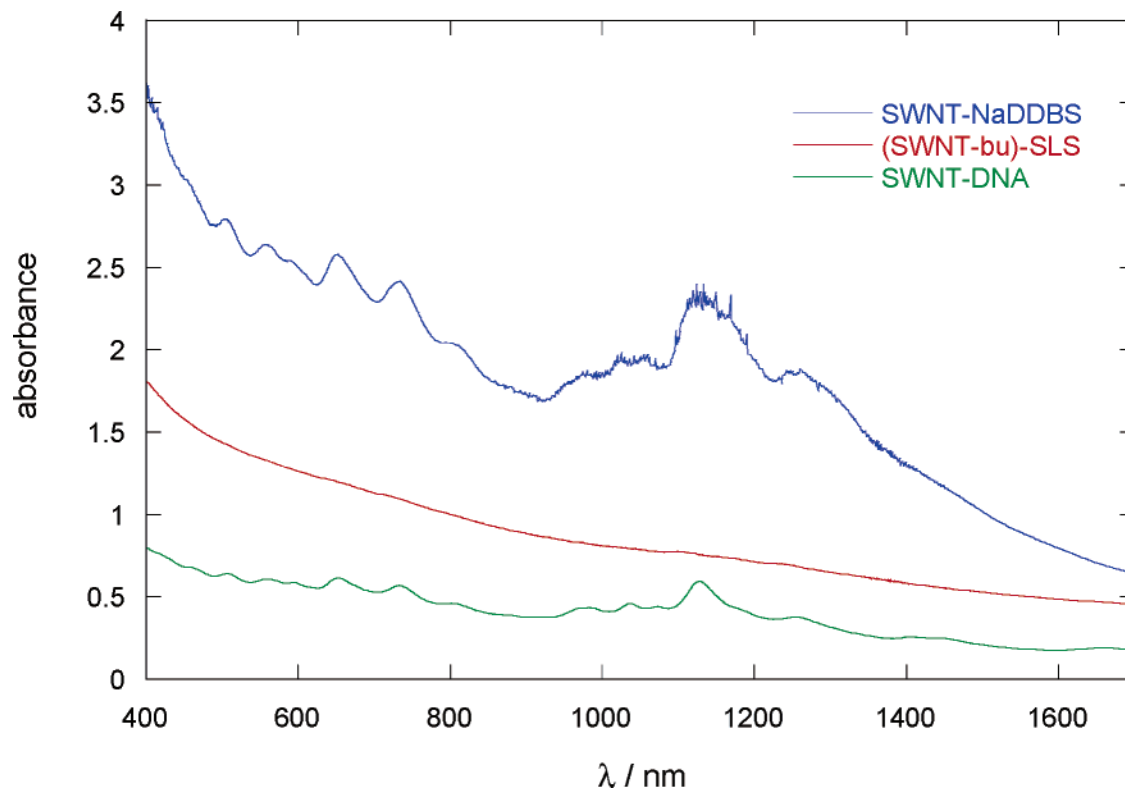


Figure 4. UV-vis-NIR spectrum of unreacted SWNTs dispersed by surfactants and wrapping polymers compared to butyl-grafted SWNT.

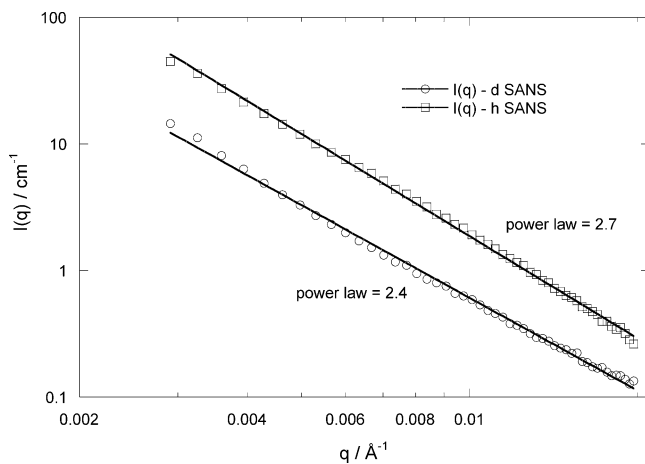


Figure 5. SANS of pure SWNT-C₄H₉ and SWNT-C₄D₉ in 1% SDS-d₂₃/D₂O with power law fits.

neutron scattering contrast as the D₂O and does not add to the scattering of the labeled SWNT.⁸ Figure 5 shows the scattering from these samples with power law fits. In both cases the power laws are between -2 and -3 , indicating either clustering or branching. On the basis of this scattering alone, it is impossible to judge whether it is due to a weak clustering or a permanent branching.

Figure 6 shows the plots of relative intensity of the two SWNT types. The plot of $(I_H(q)/(I_D(q) + I_H(q)))^{1/2}$ vs q is flat, indicating a good match in SWNT structure. The intercept gives the match point, $x_D = (\sigma_H - \sigma_S)/((\sigma_H - \sigma_S) + (\sigma_D - \sigma_S))$. A mixture is made of nanotubes at this composition (shown as a square in Figure 6) so that the scattering from eq 2 has a $Q(q)$ prefactor of zero producing only $P(q)$.

Three sets of scattering data are fit with eq 2 to produce values of both $P(q)$ and $Q(q)$ and are shown in Figure 7. The lines

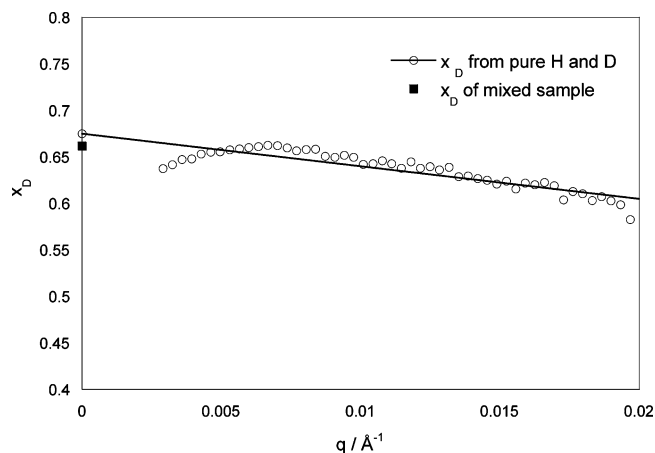


Figure 6. SANS intensity ratio of SWNT-C₄H₉/(SWNT-C₄D₉ + SWNT-C₄H₉). Intercept is the match mixture made.

are fits to the equation and accurately follow the data points. Figure 8 is a plot of the $P(q)$ and $Q(q)$ that were used in the fits. The single-particle scattering can be fit with a power law of approximately -2.5 , which is the same as the power law of whole sample. This indicates that the structure of the scattering entity is a branched collection of SWNTs. The mixing and sonication of the clustered samples do not appear to break up the clusters; instead, there appears to be mixing only at a scale larger than the individual SWNT. There is not a dynamic equilibrium that randomizes the tubes on an individual level.

The relative magnitude of the interchain scattering is small in comparison to the single-chain scattering. Therefore, the scattering at these concentrations is dominated by the scattering from clusters. The shape of the total scattering and resultant power law are good indications of the structure of the “particles” themselves. The $Q(q)$ is positive over the whole q range, which

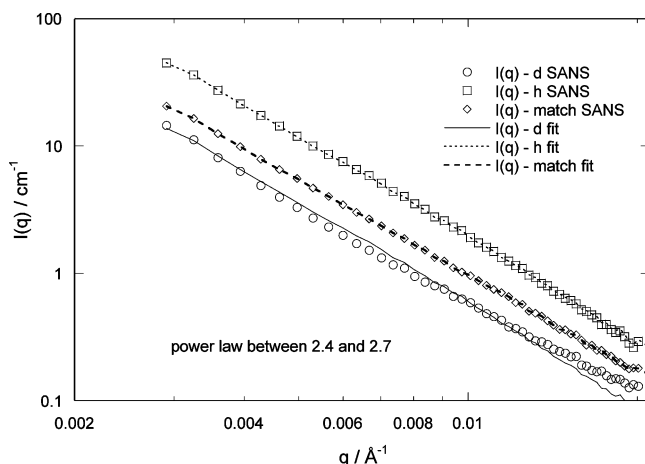


Figure 7. SANS from three three SWNT-C₄D₉ + SWNT-C₄H₉ samples with fits of the high-concentration method.

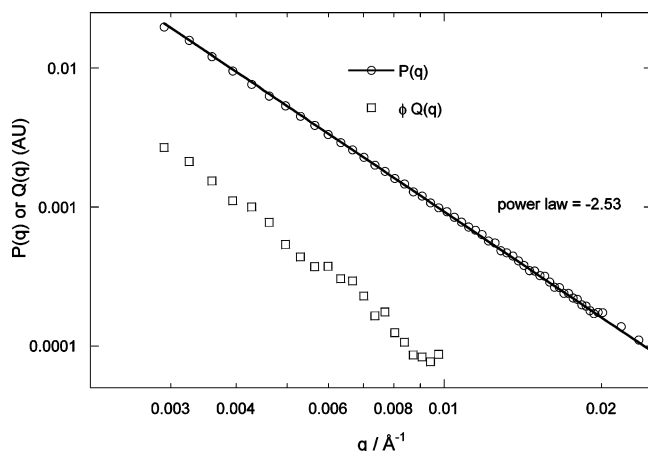


Figure 8. $P(q)$ and $S(q)$ from high-concentration fits of SANS data.

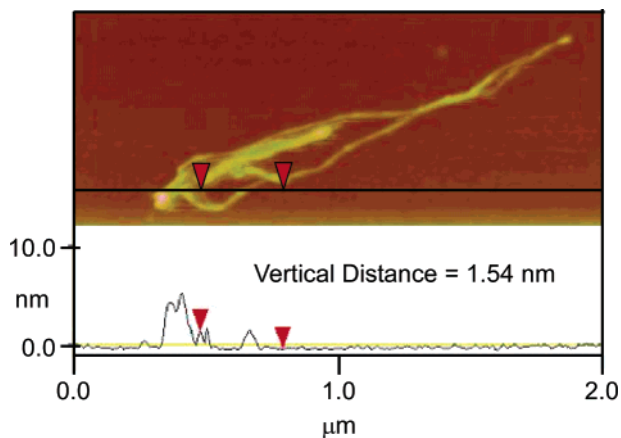


Figure 9. AFM image of grafted nanotubes showing a clustered and folded collection of SWNTs.

indicates an unfavorable thermodynamic interaction. Polymers in a good solvent have a negative $Q(q)$ and in a Θ solvent have a $Q(q) = 0$. A positive value indicates system near the point of phase separation. Since the sample was centrifuged to remove insoluble material, the remaining material in the sample is likely to be just at the point of phase separation.

Further evidence is supplied by AFM measurements. Figure 9 depicts a clustered and folded collection of SWNTs that was common for this series of samples and provides a reasonable interpretation for the data collected via the respective scattering techniques. The height measurements provided by section

analysis suggest a wrapping of multiple SWNTs or a SWNT suspended over the surface. Many AFM images were taken, and Figure 9 is typical.

As stated earlier, the covalent attachment is necessary to provide the required SANS contrast. Therefore, the structure that has been measured is only proven for the materials that result from the synthetic method that was chosen in this work. This method uses free radical chemistry that involves high-energy, random covalent attachment. Side reactions may be present that effectively “cross-link” the SWNTs into an intractable mass. Other covalent attachment schemes may produce different results.

It has to be realized that the method only works in q ranges that do not observe internal structures of the labeled SWNT. At low q values, only the composite tubes are seen as an average of the carbon tube and the labeled alkyl groups. At higher q values, sizes similar to the tube cross section would be seen. Since the cross sections have identical carbon cores, but different outer alkyl layers, the SANS in this q range would be influenced by this difference, and the high-concentration method would fail. Since the cross section is on the order of a few nanometers, only q data at the lower values are used.

The high-concentration method can potentially be applied to other types of SWNT dispersions. Other covalent attachment schemes could be used with appropriate ¹H or ²D labeling in a manner similar to the one described in this paper. Small groups of many types should be valid, but very large groups such as long grafted polymer chains will reduce the q range that is valid due to the reason stated in the previous paragraph.

A major requirement is that the labeling content does not change during the time scale of the SANS experiment. For example, two independent samples could be made with two surfactants: one containing ¹H and the other containing ²D. When mixed, the two types would quickly exchange surfactants, randomizing the types associated with the SWNTs. Therefore, the two SWNTs would become identical, and the high-contrast technique would not be applicable. Similarly, dispersions made with wrapping polymers need to have the polymers bound strongly enough such that exchange does not occur during the lifetime of the SANS data collection. The exchange rate is generally not known for such polymers, but a SANS experiment could be used to measure the exchange rate by repeating the data collection at various time intervals.

Conclusions

The high-concentration method of SANS can extract single-particle information from complicated SWNT dispersions. While SWNTs themselves do not have the hydrogens necessary for the required labeling, free radical chemistry can attach a large mass of alkyl groups to the nanotubes, producing neutron contrast between different SWNT batches. Appropriate mixtures of labeled nanotubes can be used to measure the single-particle characteristics.

The single “particle” measured in this study is not an individual nanotube; rather, it is a cluster of tubes that remains intact even when mixed with similar nanotubes and vigorously sonicated. This persistent association may be a result of the high-energy free radical chemistry involved in the labeling reaction or may be a result of high SWNT contact energy that is not overcome by the mixing methods or dispersants employed.

Acknowledgment. We gratefully acknowledge the support of Derek Ho, Charles Glinka, and Paul Butler of NCNR for aiding collection of the neutron scattering data.

References and Notes

- (1) For example: Dresselhaus, M. S.; Dai, H. *MRS Bull.* **2004**, *29*, 237–239.
- (2) Haddon, R. C.; Sippel, J.; Rinzler, A. G.; Papadimitrakopoulos, F. *MRS Bull.* **2004**, *29*, 252–259.
- (3) Roe, R.-J. Small-Angle Scattering. In *Methods of X-Ray and Neutron Scattering in Polymer Science*; Oxford University Press: New York, 2000; pp 188–193.
- (4) Schaefer, D.; Brown, J. M.; Anderson, D. P.; Zhao, J.; Chokalingam, K.; Tomlin, D.; Ilavsky, J. *J. Appl. Crystallogr.* **2003**, *36*, 553–557.
- (5) Schaefer, D. W.; Zhao, J.; Brown, J. M.; Anderson, D. P.; Tomlin, D. W. *Chem. Phys. Lett.* **2003**, *375*, 369–375.
- (6) Rols, S.; Anglaret, E.; Sauvajol, J. L.; Coddens, G.; Schober, H.; Dianoux, A. *J. Phys.: Condens. Matter* **2000**, *276*, 276–277.
- (7) Wang, H.; Zhou, W.; Ho, D. L.; Winey, K. I.; Fischer, J. E.; Glinka, C. J.; Hobbie, E. K. *Nano Lett.* **2004**, *4*, 1789–1793.
- (8) Yurekli, K.; Mitchell, C. A.; Krishnamoorti, R. *J. Am. Chem. Soc.* **2004**, *126*, 9902–9903.
- (9) Zhou, W.; Islam, M. F.; Wang, H.; Ho, D. L.; Yodh, A. G.; Winey, K. I.; Fischer, J. E. *Chem. Phys. Lett.* **2004**, *384*, 185–189.
- (10) Roe, R.-J. Small-Angle Scattering. In *Methods of X-Ray and Neutron Scattering in Polymer Science*; Oxford University Press: New York, 2000; pp 228–230.
- (11) Banerjee, S.; Hemraj-Benny, T.; Wong, S. S. *Adv. Mater.* **2005**, *17*, 17–29.
- (12) Ying, Y. M.; Saini, R. K.; Liang, F.; Sadana, A. K.; Billups, W. E. *Org. Lett.* **2003**, *5*, 1471–1473.
- (13) Certain commercial equipment and materials are identified in this paper in order to specify adequately the experimental procedure. In no case does such identification imply recommendation by NIST nor does it imply that the material or equipment identified is necessarily the best available for this purpose.
- (14) Zheng, M.; Jagota, A.; Semke, E. D.; McLean, R. S.; Lustig, S. R.; Richardson, R. E.; Tassi, N. G. *Nat. Mater.* **2003**, *2*, 338.
- (15) Zheng, M.; Jagota, A.; Strano, M. S.; Santos, A. P.; Barone, P.; Chou, S. G.; Diner, B. A.; Dresselhaus, M. S.; McLean, R. S.; Onoa, G. B.; Samsonidze, G. G.; Semke, E. D.; Usrey, M.; Walls, D. J. *Science* **2003**, *302*, 1545.

MA0527303